A ^{13}C and ^{15}N solid state NMR study of the reactions of acetone oxime adsorbed on FeZSM-5

Conrad A. Jones and Sarah C. Larsen *

Department of Chemistry, University of Iowa, Iowa City, Iowa 52242, USA

Received 8 August 2001; accepted 18 October 2001

The reactions of acetone oxime, a proposed reaction intermediate for the SCR (Selective Catalytic Reduction) of NO with propane on FeZSM-5, have been studied with ^{13}C and ^{15}N solid state MAS NMR (magic angle spinning nuclear magnetic resonance). FeZSM-5 with three different loading levels was prepared by the sublimation method. The thermal reactions of acetone [2-^{13}C] oxime adsorbed on FeZSM-5 samples with different iron loadings were monitored by ^{13}C MAS NMR by heating to the desired temperature and then cooling to room temperature for data acquisition. For the sample with the lowest iron loading (Fe/Al = 0.11), acetic acid and *N*-methyl-2-propanamine were formed by the decomposition of acetone oxime. For the samples with the higher iron loadings (Fe/Al = 0.69 and 0.91), acetone, *N*,*N*′-methyl-2,2-propanediamine, and *N*-methyl-2-propanimine were formed by the decomposition of acetone oxime. ^{15}N MAS NMR was used to investigate reactions of ^{15}NO and acetone oxime on the FeZSM-5 samples. The formation of gas phase N_2 and N_2O was observed.

KEY WORDS: FeZSM-5; SCR–HC; NO; acetone oxime; ^{15}N and ^{13}C MAS NMR

1. Introduction

Iron-exchanged zeolites, such as FeZSM-5, are active catalysts for the selective catalytic reduction of NO_x with hydrocarbons (SCR–HC) [1–9] and with ammonia (SCR–NH_3) [10–12]. Several groups have demonstrated that FeZSM-5 is much more resistant to poisoning by water than other transition metal-exchanged zeolites [1,2,4,6–9,13]. The catalytic activity of FeZSM-5 is extremely sensitive to the exchange procedure, the parent zeolite, and the pretreatment protocol.

Many studies involving catalytic activity measurements often coupled with temperature programmed desorption (TPD) techniques have yielded important information about the conversion, kinetics and surface species of the NO_x SCR–HC reaction on FeZSM-5 [1,2,4–9,14–18]. In addition, electron paramagnetic resonance (EPR) spectroscopy [18–22], Mössbauer spectroscopy [23–25] and X-ray absorption spectroscopy [13,26] have been used to determine the electronic structure of the active iron centers in several different iron-exchanged zeolites. Isolated iron centers and iron oxide aggregates have been identified using these techniques. Spectroscopic studies of surface species formed on FeZSM-5 under SCR–HC reaction conditions have been conducted using Fourier Transform Infrared (FTIR) spectroscopy [5,7,8,16–18].

The mechanism for the SCR–HC reaction on FeZSM-5 remains controversial. Recently, Chen and Sachtler showed that a nitrogen-containing surface species was formed on FeZSM-5 and that the surface species reacted with NO_2 to form N_2 [5,7]. Analogous to their work on the SCR–HC of NO_x on CuZSM-5, Sachtler and coworkers used FTIR and mass spectrometry to study the reactivity of various adsorption complexes on FeZSM-5 [7]. They found that NO and O_2 formed NO_y complexes ($y > 2$) on FeZSM-5 that subsequently reacted with hydrocarbon to form a nitrogen-containing deposit [5,7]. The nitrogen-containing deposit reacted with NO to form N_2. They suggested that the nitrogen-containing deposit might be an organic nitro- or nitroso- compound that can undergo spontaneous isomerization to an oxime [14]. Acetone oxime has been previously proposed as an intermediate for SCR–HC of NO_x with propane on CuZSM-5 [5,7,27–33]. The identification of the NO_y complex and the nitrogen-containing deposit was not unambiguously determined in the FTIR studies.

Solid state nuclear magnetic resonance (NMR) has proven to be a powerful non-invasive structural probe and a unique technique that provides insight into physical and chemical processes that may be inaccessible by other spectroscopic methods. NMR studies have demonstrated numerous applications of NMR in obtaining valuable structural and mechanistic information, in monitoring catalytic reactions and in studying surface chemistry on catalysts, such as zeolites [17,34,35], and supported metal catalysts [36,37]. Previously, we have demonstrated the utility of ^{13}C and ^{15}N magic angle spinning (MAS) NMR for studying SCR catalysts [34,38].

* To whom correspondence should be addressed.
E-mail: sarah-larsen@uiowa.edu

1011-372X/02/0300-0243/0

In this study, solid state ^{13}C and ^{15}N NMR spectroscopy was used to study the reactions of the proposed SCR–HC reaction intermediate, acetone oxime, on FeZSM-5. Three FeZSM-5 samples with different iron loadings were prepared using the sublimation method [5,9]. The decomposition of acetone [2-^{13}C] oxime on FeZSM-5 was monitored using ^{13}C NMR methods. The interaction of acetone oxime with ^{15}NO on FeZSM-5 was investigated with ^{15}N solid state NMR techniques. Through the combination of ^{13}C and ^{15}N NMR and isotopic labeling, the carbon- and/or nitrogen-containing adsorbed surface species and/or gaseous products formed under conditions of thermodynamic equilibrium were identified.

2. Experimental section

2.1. Synthesis and characterization of FeZSM-5

HZSM-5 catalyst was prepared by exchanging the Na^+ in NaZSM-5 (Zeolyst, Si/Al = 15) with NH_4^+ which subsequently decomposed to produce NH_3 and the Brønsted site. The exchange was achieved by soaking 10 g of NaZSM-5 in 500 ml of 0.1 M NH_4NO_3 (Baker) for 24 h, followed by drying the product in an oven at 353 K for 2 h. The final step was to heat the sample to 400 °C in oxygen for 24 h.

Iron-exchanged ZSM-5 (FeZSM-5) was prepared by the sublimation method according to Lobree *et al.* [9]. 1.6 (0.8, 0.4) g of $FeCl_3 \cdot H_2O$ (Aldrich) and 5 g of HZSM-5 were ground in a mortar and pestle contained in a glove bag of nitrogen. The yellow mixture was then transferred under a nitrogen atmosphere to a quartz calcination tube. The calcination tube containing the sample was placed in a furnace and was heated under argon to 310 °C, the sublimation temperature of $FeCl_3 \cdot H_2O$. The sample was held at 310 °C for 4 h. The orange red sample was filtered, washed with deionized water and dried at 80 °C overnight. Samples with three different iron loadings were prepared. The form of sample identification that will be used throughout this paper is *zeolite-exchange level* (%) (*i.e.*, FeZSM-5-11 has an iron exchange level of 11%). The exchange level was calculated by taking the Fe/Al ratio determined by inductively coupled plasma-atomic emission spectroscopy (ICP–AES) and multiplying by 100 ((Fe/Al) × 100 = % Fe exchange.) Samples with ion-exchange levels of 11, 69 and 91% were prepared. The corresponding Fe wt% are 0.61, 3.44 and 4.30. XRD (X-Ray Diffraction) patterns obtained after the exchange procedure did not show the presence of any other phases in these samples.

2.2. Synthesis of labeled acetone oxime

The ^{13}C (C-2 labeled) acetone oxime was synthesized according to procedures in the literature [34,39]. The synthesized ^{13}C labeled acetone oxime was characterized by FTIR and ^{1}H and ^{13}C solution-state NMR. The synthesized labeled acetone oxime product was found to be identical to the acetone oxime (ACROS) which was used as a standard.

2.3 Preparation of samples for NMR

FeZSM-5, typically 0.3 g, was impregnated *ex situ* with an aqueous acetone oxime solution. Samples with (acetone oxime)/Fe ratios of 4:1 were prepared. All the samples, preadsorbed with acetone oxime, were dried at room temperature to avoid decomposition and then were loaded into pyrex sample tubes. The pyrex sample tubes were outgassed *in situ* on a vacuum rack, and then nitric oxide was introduced into the sample tubes on the vacuum rack by immersing the sample tubes in liquid nitrogen. A torch was used to seal the pyrex sample tubes. Nitric-^{15}N oxide (98% ^{15}N, Cambridge Isotopes) was the limiting reagent when acetone oxime and NO were both added to samples of FeZSM-5. Incremental off-line heating of the samples was used and the reaction temperature was controlled by an Omega (CN-76000) programmable temperature controller. Samples were then cooled to room temperature for data acquisition. The sealed sample tubes were placed in Chemagnetics 7.5 mm (o.d.) pencil rotors for magic angle spinning (MAS) NMR measurements.

2.4. NMR Spectroscopy

The ^{13}C and ^{15}N NMR spectra were obtained using a wide bore Bruker MSL-300 NMR spectrometer operating at 75.470 MHz and 30.425 MHz for ^{13}C and ^{15}N, respectively. A Chemagnetics double-channel 7.5 mm pencil MAS probe was used to spin rotors loaded with the sealed samples at 4.0–5.0 kHz at the magic angle. Single pulse direct excitation was used for ^{15}N, with $\pi/2$ pulse widths of 5.75 μs. Recycle delay was 2 s for ^{15}N and 25 000 scans were typically acquired. Several pulse sequences, such as cross polarization (CP), single pulse excitation with high power proton decoupling (46 kHz), and single pulse direct excitation were used for ^{13}C NMR signal acquisition with the following parameters: CP, contact time 1.5 ms, recycle delay 2 s, typical 90° pulse length 5.5 μs; single pulse direct excitation, recycle delay 2 s, $\pi/2$ pulse of 5.5 μs. Typically 10 000 and 25 000 scans were acquired for ^{13}C and ^{15}N NMR experiments, respectively. A line broadening of 50 Hz was used for ^{15}N and ^{13}C spectra. Solid adamantane mixed with KBr (28.5 ppm) and saturated $NH_4{}^{15}NO_3$ (−4 ppm) were used as external chemical shift standards for ^{13}C and ^{15}N, respectively. All of the chemical shifts for ^{13}C and ^{15}N are reported relative to TMS and to CH_3NO_2, respectively. All of the NMR spectra were acquired at 25 °C.

3. Results

3.1. Adsorption of acetone oxime on FeZSM-5

The ^{13}C CP/MAS NMR spectra of sealed samples of acetone [2-^{13}C] oxime adsorbed on (a) FeZSM-5-11; (b) FeZSM-5-69; and (c) FeZSM-5-91 at room temperature are shown in figure 1. A peak at 169 ppm in figure 1(a) is assigned to the C-2 labeled carbon of adsorbed acetone oxime. The peak at 169 ppm shifts to 164 and 163 ppm and broadens considerably in the spectra shown in figure 1(b), (c) as the iron exchange level increases. Spinning sidebands (indicated by the asterisks) are also present in the spectra in figure 1. Solid synthesized acetone [2-^{13}C] oxime has a chemical shift of 156 ppm. In our previous work, the chemical shift of acetone [2-^{13}C] oxime adsorbed on HZSM-5 and CuZSM-5 was found to range from 164 to 172 depending on the coverage and on the interaction of the acetone oxime with the zeolite [34]. Similar effects for adsorbed carbonyl compounds have been observed previously [40,41]. The broadening of the NMR peak assigned to the C-2 carbon of acetone oxime can be attributed to an increase in the amount of paramagnetic iron present in the sample as the iron loading is increased.

3.2. Decomposition of acetone oxime adsorbed on FeZSM-5

The ^{13}C CP/MAS NMR spectrum of a sealed sample of acetone [2-^{13}C] oxime adsorbed on FeZSM-5-11 at room temperature is shown in figure 2(a). The peak at 169 ppm is assigned to the C-2 labeled carbon of adsorbed acetone oxime as discussed above. After heating the sample to 150 °C (250 °C), followed by cooling to room temperature for data acquisition, the ^{13}C CP/MAS NMR spectra shown in figure 2(b),(c) were acquired. After heating to 150 °C, new peaks at 180 and 197 ppm appear and the peak at 169 ppm due to acetone oxime decreases in intensity. The peak at 180 ppm is assigned to the carbonyl carbon of acetic acid as discussed in previous work [34]. The peak at 197 ppm is assigned to *N*-methyl-2-propanimine by comparison with NMR data for similar imines in the literature [40,42]. After heating to 250 °C, peaks at 180, 23 and 17 ppm are observed. The peak at 169 due to acetone oxime is no longer present presumably because the acetone oxime has completely reacted. The peak at 180 ppm assigned to acetic acid increases in intensity relative to the spectrum in figure 2(b). The peaks at 23 and 17 ppm are due to methyl type carbon atoms possibly due to cleavage chemistry of the acetic acid or the *N*-methyl-2-propanimine.

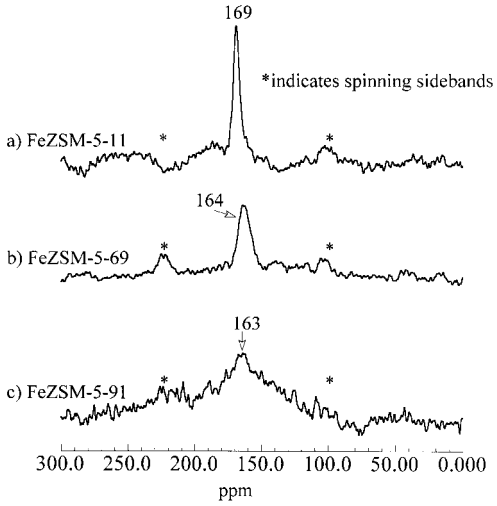

Figure 1. ^{13}C CP/MAS NMR spectra of acetone [2-^{13}C] oxime adsorbed on (a) FeZSM-5-11; (b) FeZSM-5-69; and (c) FeZSM-5-91. Asterisks denote spinning sidebands. Spectra were acquired at room temperature. NS (number of scans acquired) was (a) 10 000; (b) 10 000; and (c) 40 000. Line broadening = 100 Hz.

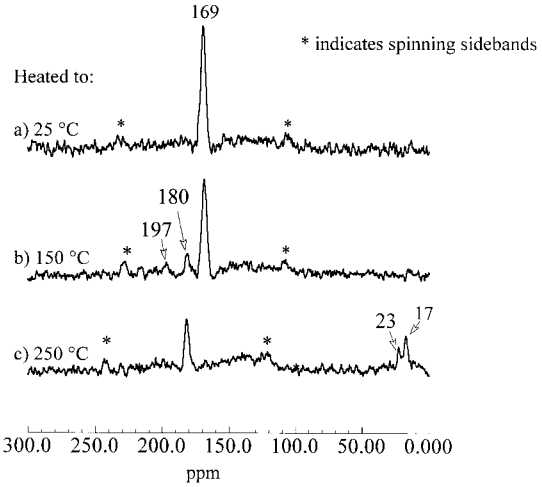

Figure 2. ^{13}C CP/MAS NMR spectra of acetone [2-^{13}C] oxime adsorbed on FeZSM-5-11 before and after heating to the indicated temperatures. Asterisks denote spinning sidebands. Spectra were acquired at room temperature after the sealed sample was heated to: (a) 25 °C; (b) 150 °C; (c) 250 °C. NS (number of scans acquired) was 10 000. Line broadening = 50 Hz.

Figure 3 shows the ^{13}C single pulse with proton decoupling NMR spectra acquired after a sealed sample of acetone [2-^{13}C] oxime adsorbed on FeZSM-5-69 was heated from room temperature to 150 °C and then 250 °C and cooled to room temperature for data acquisition. A peak at 164 ppm is observed and is assigned to the C-2 labeled carbon of adsorbed acetone oxime. The adsorbed acetone oxime peak is substantially broader than the peak for acetone oxime on FeZSM-5-11 and this is due to the increased amount of paramagnetic iron (Fe^{+3}) present in the higher loading sample. After heating to 150 °C, a peak at 211 ppm is observed. The peak at 211 ppm is assigned to the C-2 carbon of adsorbed acetone consistent with previous work in the literature [34,40,41]. After heating to 250 °C and cooling to room temperature for data acquisition, peaks at 211,

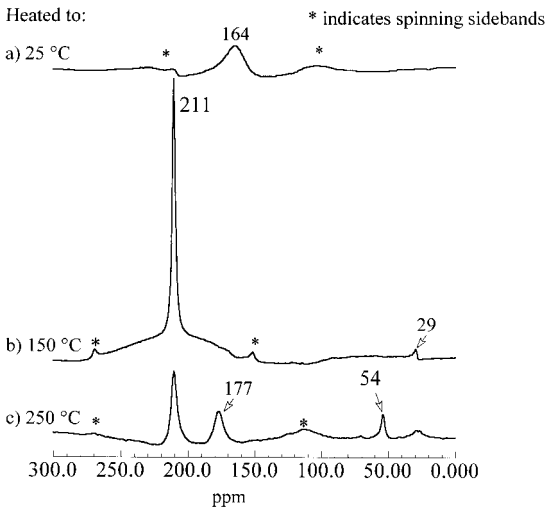

Figure 3. ^{13}C single pulse with decoupling MAS NMR spectra of acetone [2-^{13}C] oxime adsorbed on FeZSM-5-69 before and after heating to the indicated temperatures. Asterisks denote spinning sidebands. Spectra were acquired at room temperature after the sealed sample was heated to: (a) 25 °C; (b) 150 °C; (c) 250 °C. NS (number of scans acquired) was 10 000. Line broadening = 100 Hz.

177, 54 and 29 ppm are observed in the single pulse ^{13}C NMR spectrum shown in figure 3(c). The peak at 177 ppm is assigned to acetic acid as discussed above and as in previous work [34]. The peak at 54 ppm is assigned to the primary diamine, *N*,*N*′-methyl-2,2-propanediamine, analogous to Biaglow and coworkers, who previously found that 2-propanimine reacted with NH_3 to produce a primary diamine, which had a ^{13}C chemical shift of 54 ppm [40]. The peak at 29 ppm is assigned to a methyl carbon group.

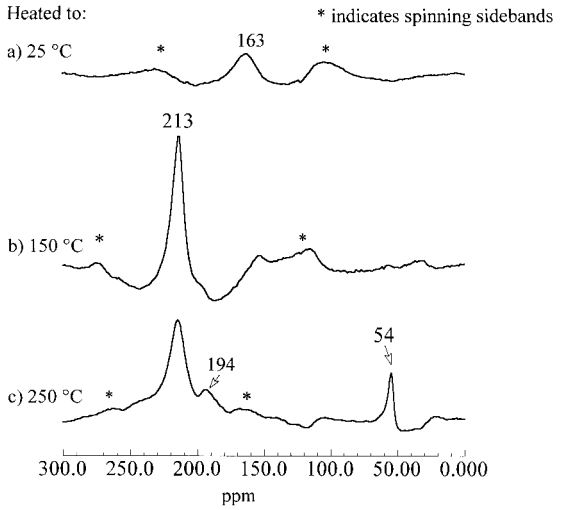

Figure 4. ^{13}C single pulse with decoupling MAS NMR spectra of acetone [2-^{13}C] oxime adsorbed on FeZSM-5-91 before and after heating to the indicated temperatures. Asterisks denote spinning sidebands. Spectra were acquired at room temperature after the sealed sample was heated to: (a) 25 °C; (b) 150 °C; (c) 250 °C. NS (number of scans acquired) was 10 000. Line broadening = 100 Hz.

The ^{13}C single pulse with decoupling NMR spectra of acetone [2-^{13}C] oxime adsorbed on Fe-ZSM-5-91 are shown in figure 4(a)–(c). The NMR spectrum of adsorbed acetone [2-^{13}C] oxime is quite broad and large spinning sidebands are present in the spectrum shown in figure 4(a). The spectrum is extensively broadened due to the high concentration of iron species. After heating the sample to 150 °C and cooling to room temperature for data acquisition, a peak at 213 is observed and can be assigned to the C-2 carbon of acetone [40–42]. Upon further heating of the sample to 250 °C, peaks at 194 and 54 ppm are also present as shown in figure 4(c). These peaks are assigned to *N*-methyl-2-propanimine and *N*-methyl-2,2-propanediamine analogous to previous work [40] and as discussed above.

3.3. Reaction of acetone oxime and ^{15}NO on FeZSM-5

The ^{15}N MAS NMR spectra of adsorbed acetone oxime-^{14}N with ^{15}NO on FeZSM-5-69 are shown in figure 5(a)–(c). The ^{15}N peaks at −145 and −232 ppm in figure 5(a) are assigned to N_2O (central N at *ca.* −148 ppm and terminal N at *ca.* −232 to −235 ppm) [3,34,38,43]. After heating to 150 °C, the formation of N_2 (−72 ppm) is also observed [3,34,38,43]. After heating to 250 °C, only one peak due to N_2 is observed in the ^{15}N NMR spectrum as shown in figure 5(c). The ^{15}N NMR spectra of adsorbed acetone oxime-^{14}N with ^{15}NO on FeZSM-5-11 (not shown) exhibit NMR spectra very similar to those observed for the FeZSM-5-69 sample and shown in figure 5(a)–(c). The ^{15}N NMR spectra of

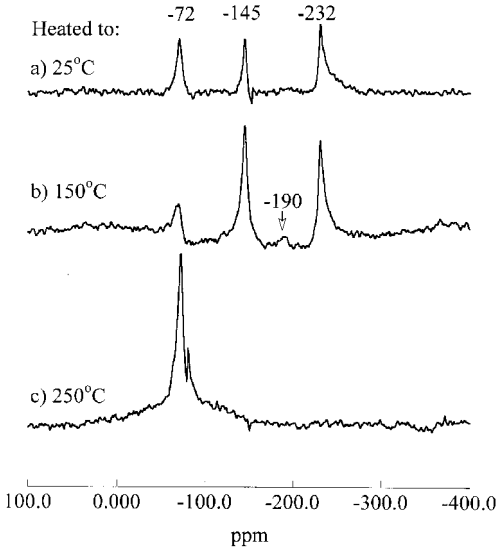

Figure 5. ^{15}N single pulse MAS NMR spectra of acetone oxime and ^{15}NO adsorbed on FeZSM-5-69 before and after heating to the indicated temperatures. Asterisks denote spinning sidebands. Spectra were acquired at room temperature after the sealed sample was heated to: (a) 25 °C; (b) 150 °C; (c) 250 °C. NS (number of scans acquired) was 25 000. Line broadening = 50 Hz.

adsorbed acetone oxime-^{14}N with ^{15}NO on FeZSM-5-91 (not shown) were characterized by very poor signal to noise and weak N_2 and N_2O peaks.

4. Discussion

4.1. Adsorption of acetone oxime on FeZSM-5 with different iron loadings

The chemical shift of adsorbed acetone-[2-^{13}C]- oxime depends on the coverage and on the identity and loading of the exchangeable cation in cation-exchanged zeolites. In related work, we observed that the chemical shift of acetone-[2-^{13}C]- oxime adsorbed on HZSM-5 and CuZSM-5 shifted downfield relative to the chemical shift of solid synthesized acetone-[2-^{13}C]- oxime [34]. The shift depended not only on the identity of the exchangeable cation but on the coverage of the acetone oxime. A similar coverage dependence has been observed for acetone adsorbed on zeolites [40–42]. The chemical shift variation was attributed to H-bonding of the adsorbate with Brønsted acid sites on the zeolite [41,42].

In this study, the chemical shift of adsorbed acetone oxime depends on the iron exchange level of the zeolite. A plot of the ^{13}C chemical shift for acetone-[2-^{13}C]-oxime adsorbed on FeZSM-5 versus the iron exchange level is shown in figure 6. The acetone oxime/cation site loading is approximately 4. The chemical shifts for acetone oxime absorbed on HZSM-5 (172 ppm, loading 1 acetone oxime/Brønsted site) and CuZSM-5-60 (164 ppm, loading 3 acetone oxime/cation site) have been included in figure 6 for comparison. The data in figure 6 indicates that the chemical shift of adsorbed acetone oxime depends linearly on the exchange level of the exchanged cation. The best fit line through the data is shown in figure 6 ($y = 170.88 - 0.096933x$; $R = 0.97$). The data suggests that as the exchange level of the zeolite increases to ~150% based on Fe/Al ratio, the chemical shift of the adsorbed acetone oxime approaches the value for pure solid acetone oxime, 156 ppm [34]. The Brønsted acid sites in HZSM-5 are replaced by iron cations during the exchange process. Therefore, the lower the exchange level, the more Brønsted sites that are available for adsorption and the greater the increase of the ^{13}C chemical shift. This chemical shift dependence with exchange level supports the idea that the variation in the chemical shift of the adsorbed acetone oxime is due to interactions with the Brønsted acid site protons [46].

4.2. Decomposition of acetone oxime on FeZSM-5 with different iron loadings

As shown in Scheme 1, adsorbed acetone oxime is decomposed by two different pathways depending on the acidity of the zeolite host [34]. Previously, we found that for acetone oxime adsorbed on CuZSM-5, the primary decomposition route was hydrolysis to form acetone and hydroxylamine (Scheme 1A). For acetone oxime adsorbed on HZSM-5, the decomposition followed the acid-catalyzed Beckman rearrangement followed by hydrolysis to form acetic acid and methylamine as shown in Scheme 1B. In this study, for acetone oxime adsorbed on FeZSM-5-11, the sample with the lowest iron loading, the decomposition of acetone oxime yields acetic acid and a small amount of *N*-methyl-2-propanimine. This is consistent with the fact that this sample contains a large number of Brønsted acid sites and therefore the acid catalyzed pathway is favored. At higher iron loadings, the decomposition

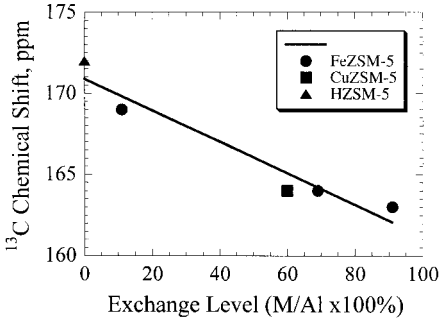

Figure 6. Plot of the ^{13}C chemical shifts obtained from the single pulse ^{13}C MAS NMR spectra of acetone-[2-^{13}C]-oxime adsorbed on FeZSM-5 *versus* the iron exchange level for each of the samples used in this study. The ^{13}C chemical shifts for acetone-[2-^{13}C]-oxime adsorbed on HZSM-5 and CuZSM-5 from previous work [34] are also included. The acetone oxime coverage was approximately 4 acetone oxime molecules/Brønsted acid or iron site for the iron-exchanged samples. The acetone oxime coverage was 3 acetone oxime molecules/copper site for CuZSM-5-60 and 1 acetone oxime molecule/Brønsted acid site for HZSM-5.

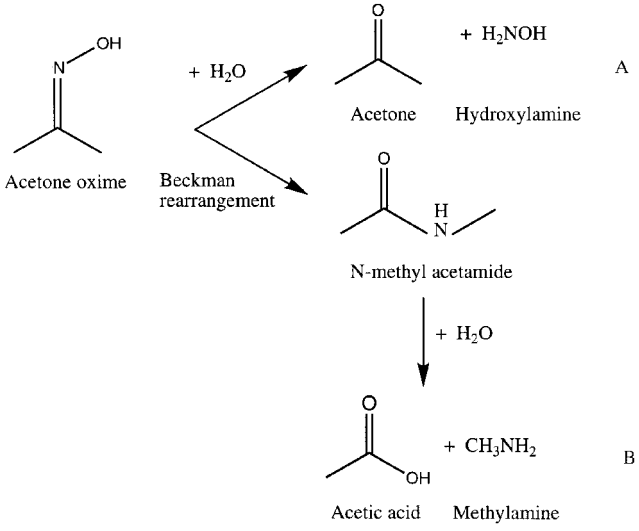

Scheme 1.

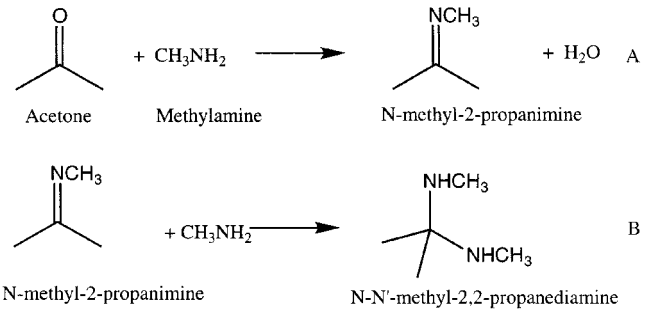

Scheme 2.

of acetone oxime yields mainly acetone along with smaller amounts of *N*-methyl-2-propanimine and *N*,*N*′-methyl-2,2-propanediamine. The reactions describing the formation of *N*-methyl-2-propanimine and *N*,*N*′-methyl-2,2-propanediamine are shown in Scheme 2. The *N*,*N*′-methyl-2,2-propanediamine is formed by reaction of *N*-methyl-2-propanimine with methylamine. Analogously, Biaglow *et al.* observed the formation of 2-propanediamine after reaction of 2-propanimine with excess ammonia [40]. Therefore the results show that for the lowest iron loading the sample reacts similarly to HZSM-5 while at the higher iron loadings the reactivity is similar to that of copper-exchanged ZSM-5 samples. The formation of the diamine by the route shown in Scheme 2 has not been previously observed in cation-exchanged zeolites.

4.3. Reaction of acetone oxime with ^{15}NO on FeZSM-5

^{15}N MAS NMR (figure 5) showed that N_2 and N_2O were produced in a sealed sample of ^{15}NO and adsorbed acetone oxime-^{14}N on FeZSM-5. The N_2 peak increases in intensity as the sample is heated to 250 °C suggesting that the N_2O is converted into N_2 as has been well-documented previously [4,18,47,48]. Similar results were observed for samples with iron exchange levels of 11 and 69%. For the highest iron loading the signal to noise ratio was extremely poor. A mechanism for the formation of N_2O and N_2 from acetone oxime was previously suggested by Adelman *et al.* and is shown in Scheme 3 [30]. In the proposed scheme, NO reacts with acetone oxime to form a cation complex which then decomposes to form N_2O. Further reaction leads to the formation of acetone, N_2 and water.

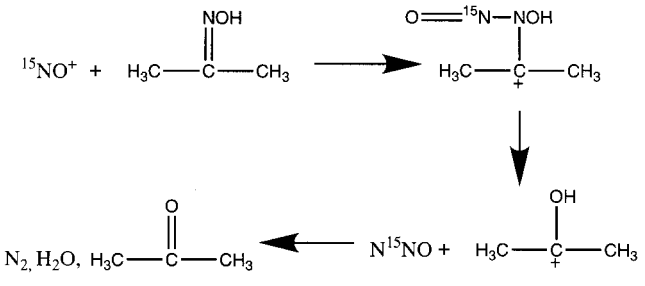

Scheme 3.

Conclusions

Solid state NMR was utilized to investigate the reactions of acetone oxime and NO adsorbed on FeZSM-5 with different iron exchange levels. The reactions of acetone oxime on FeZSM-5 were monitored using ^{13}C and ^{15}N NMR. The predominant reaction path for acetone oxime depends on the exchange level of the FeZSM-5 samples. For the lowest iron exchange level examined (11%), acetone oxime primarily decomposes to acetic acid and hydroxylamine. For the higher exchange levels (69 and 91%, respectively) acetone oxime decomposes to form acetone, *N*-methyl-2-propanimine and *N*,*N*′-methyl-2,2-propanediamine. Acetone oxime reacts with gas phase ^{15}NO on FeZSM-5 to form a new N–N bond. ^{13}C and ^{15}N NMR were utilized to identify products formed from reactions of acetone oxime and NO. The results demonstrate the potential of solid state NMR for studying surface species that may be important catalytic intermediates.

Acknowledgments

Acknowledgement is made to the Center for Global and Regional Environmental Research at the University of Iowa and to Dr. Russell Larsen and Dr. Donald Stec for assistance with experiments.

References

[1] X. Feng and W.K. Hall, J. Catal. 166 (1997) 368.
[2] X. Feng and W.K. Hall, Catal. Lett. 41 (1996) 45.
[3] V.M. Mastikhin and S.V. Filimonova, J. Chem. Soc., Faraday Trans. 88 (1992) 1473.
[4] M. Kogel, R. Monnig, W. Schweiger, A. Tissler and T. Turek, J. Catal. 182 (1999) 470.
[5] H.-Y. Chen and W.M.H. Sachtler, Catal. Lett. 50 (1998) 125.
[6] H.-Y. Chen and W.M.H. Sachtler, Catal. Today 42 (1998) 73.
[7] H.-Y. Chen, T.V. Voskoboinikov and W.M.H. Sachtler, J. Catal. 180 (1998) 171.
[8] L.J. Lobree, I. Hwang, J.A. Reimer and A.T. Bell, Catal. Lett. 63 (1999) 233.
[9] L.J. Lobree, I. Hwang, J.A. Reimer and A.T. Bell, J. Catal. 186 (1999) 242.
[10] R.Q. Long and R.T. Yang, J. Catal. 188 (1999) 332.
[11] R.Q. Long and R.T. Yang, J. Am. Chem. Soc. 121 (1999) 5595.
[12] A.Z. Ma and W. Grunert, Chem. Commun. (1999) 71.
[13] R. Joyner and M. Stockenhuber, J. Phys. Chem. B 103 (1999) 5963.
[14] H.-Y. Chen, T. Voskoboinikov and W.M.H. Sachtler, J. Catal. 186 (1999) 91.
[15] T.V. Voskoboinikov, H.-Y. Chen and W.M.H. Sachtler, Applied Catal. B: Environmental 19 (1998) 279.
[16] K. Hadjiivanov, H. Knozinger, B. Tsyntsarski and L. Dimitrov, Catal. Lett. 62 (1999) 35.

[17] I.O.Y. Liu, N.W. Cant, M. Kogel and T. Turek, Catal. Lett. 63 (1999) 241.
[18] E.-M. El-Maki, R.A. van Santen and W.M.H. Sachtler, J. Catal. 196 (2000) 212.
[19] A.V. Kucherov, T.N. Montreuil, T.N. Kucherova and M. Shelef, Catal. Lett. 56 (1998) 173.
[20] A.V. Kucherov and A.A. Slinkin, Zeolites 8 (1988) 110.
[21] D. Goldfarb, M. Bernardo, K.G. Strohmaier, D.E.W. Vaughan and H. Thomann, J. Am. Chem. Soc. 116 (1994) 6344.
[22] H.-T. Lee and H.-K. Rhee, Catal. Lett. 61 (1999) 71.
[23] W.K. Hall, X. Feng, J. Dumesic and R. Watwe, Catal. Lett. 1998 (1998) 13.
[24] M. Mauvezin, G. Delahay, B. Coq, S. Kieger, J.C. Jumas and J. Olivier-Fourcade, J. Phys. Chem. B 105 (2001) 928.
[25] A.M. Volodin, K.A. Dubkov and A. Lund, Chem. Phys. Lett. 333 (2001) 41.
[26] P. Marturano, L. Drozdova, A. Kogelbauer and R. Prins, J. Catal. 192 (2000) 236.
[27] E.V. Rebrov, A.V. Simakov, N.N. Sazonova and E.S. Stoyanov, Catal. Lett. 58 (1999) 107.
[28] E.V. Rebrov, A.V. Simakov, N.N. Sazonova, V.A. Rogov and G.B. Barannik, Catal. Lett. 51 (1998) 27.
[29] B.J. Adelman, T. Beutel, G.-D. Lei and W.M.H. Sachtler, J. Catal. 158 (1996) 327.
[30] B.J. Adelman, T. Beutel, G.-D. Lei and W.M.H. Sachtler, Appl. Catal. B 11 (1996) L1.
[31] T. Beutel, B.J. Adelman and W.M.H. Sachtler, Catal. Lett. 37 (1996) 125.
[32] T. Beutel, J. Sarkany, G.-D. Lei, J.Y. Yan and W.M.H. Sachtler, J. Phys. Chem. 100 (1996) 845.
[33] T. Beutel, B.J. Adelman, G.-D. Lei and W.M.H. Sachtler, Catal. Lett. 32 (1995) 83.
[34] J. Wu and S.C. Larsen, J. Catal. 182 (1999) 244.
[35] J.F. Haw, *NMR Techniques in Catalysis*, eds. A.T. Bell and A. Pines, (1994) 139.
[36] C.P. Slichter, Ann. Rev. Phys. Chem. 37 (1986) 25.
[37] T.M. Duncan, Colloids Surf. 45 (1990) 11.
[38] J. Wu and S.C. Larsen, Catal. Lett. 70 (2000) 43.
[39] W.L. Semon, Organic Synthesis coll. Vol. 1 (1941) 318.
[40] A.I. Biaglow, J. Sepa, R.J. Gorte and D. White, J. Catal. 151 (1995) 373.
[41] T. Xu, E.J. Munson and J.F. Haw, J. Am. Chem. Soc. 116 (1994) 1962.
[42] T. Xu, J. Zhang and J.F. Haw, J. Am. Chem. Soc. 117 (1995) 3171.
[43] V.M. Mastikhin, I.L. Mudrakovsky and S.V. Filimonova, Chem. Phys. Lett. 149 (1988) 175.
[44] S. Hu and T.M. Apple, J. Catal. 158 (1996) 199.
[45] M. Witanowski, L. Stefaniak and G.A. Webb, in: *Annual Reports on NMR Spectroscopy*, Vol. 25, ed. G.A. Webb (Academic Press, San Diego 1993).
[46] W.O.N.J. Parker, Magnet. Resonance Chem. 37 (1999) 433.
[47] Y.F. Chang and J.G. McCarty, Catal. Lett. 34 (1995) 163.
[48] V.I. Sobolev, G.I. Panov, A.S. Kharitonov, W.N. Romannikov, A.M. Volodin and K.G. Ione, J. Catal. 139 (1993) 435.